13,18

# Mode bistability of plasmons and dispersive jump in a structure with two graphene layers

© A.M. Shutyi, D.I. Sementsov, S.V. Eliseeva

Ulyanovsk State University,
Ulyanovsk, Russia

E-mail: shuty@mail.ru

Received December 20, 2021
Revised February 10, 2022
Accepted February 14, 2022

Plasmon modes in a symmetric structure consisting of two layers of inverted graphene separated by a dielectric barrier layer and their dispersion properties are studied for various parameters of the barrier layer. The occurrence of a bifurcation of the splitting of the branch of the dispersion dependence, which leads to the appearance of bistability and a dispersion jump with a change in the stability of the branches included in the bistability, is found. The plasmonic modes belonging to the two branches of the bistable state differ in the gain increment and phase velocity, and their group velocities are opposite in sign.

**Keywords:** inverted graphene, three-layer structure, branching bifurcation, modal bistability, amplifying modes, dispersion dependence jump.

DOI: 10.21883/PSS.2022.06.53839.259

## 1. Introduction

Graphene and various structures based thereon have been recently considered as one of the most promising photonics materials. Retardation and control of dispersion characteristics of the waves, its phase and group velocity can be performed in the said structures by external electric and magnetic fields and the temperature as well. At terahertz frequencies, the graphene-based structures have a strong plasmon response due to unique electronic and optical properties of graphene, which are correlated to a zero-gap linear energy spectrum of charge carriers [1–12]. Generation of plasma waves in the graphene structures allows concentrating the electromagnetic field near graphene layers and substantially increasing efficiency of its interaction with the structure.

The papers [13–17] have shown that the THz radiation may be enhanced by graphene with inverted distribution of the charge carriers (electrons and holes). When optical pumping is at a certain threshold value, the inversion of the charge carriers in graphene results in negative high-frequency conductivity [18]. The presence of negative differential conductivity may lead to stimulated generation of the THz plasmons in graphene [19]. In the structure consisting of two parallel graphene layers, which are divided by a thin dielectric barrier layer, the electromagnetic fields propagating in these layers of plasmons interact with each other, thereby leading to generation of a single plasmonic mode [20–24].

The present paper studies the gaining plasmonic modes in the symmetrical structure with two graphene layers at different parameters of the barrier layer. Construction and analysis of dispersion dependences of antisymmetric plasmonic modes made it possible to detect bifurcation of splitting of a dispersion branch, thereby resulting in modal bistability and a dispersive jump, which occurs when stability of bistable states changes. Conditions of implementation of this effect have been revealed.

## 2. Initial equations

Let us consider a planar symmetric structure consisting of two monolayers of inverted graphene, which are divided by the dielectric barrier layer $d$ thick and covered by dielectric liners. Dielectric permittivities (DP) of the barrier layer $\varepsilon_b$ and the liners $\varepsilon_c$ do not depend on the frequency and are real values. The graphene layers have the same inversion of population of vacant charge carriers created, which can be provided by symmetric direct or diffusive pumping of each of the graphene layers [25,26]. For inverted distribution of the charge carriers, a surface dynamic distribution of graphene is determined using the expression [18,27,28]:

$$\frac{\sigma(\omega)}{\sigma_0} = \frac{8k_{\mathrm{B}}T\tau}{\pi\hbar(1-i\omega\tau)}\ln\left[1+\exp\left(\frac{E_{\mathrm{F}}}{k_{\mathrm{B}}T}\right)\right] + \tanh\left(\frac{\hbar\omega-2E_{\mathrm{F}}}{4k_{\mathrm{B}}T}\right) - \frac{4\hbar\omega}{i\pi}\int\limits_0^\infty \frac{G(\varepsilon,E_{\mathrm{F}})-G(\hbar\omega/2,E_{\mathrm{F}})}{(\hbar\omega)^2-4\varepsilon^2}\,d\varepsilon, \tag{1}$$

where the function

$$G(\varepsilon,E_{\mathrm{F}}) = \frac{\sinh(\varepsilon/k_{\mathrm{B}}T)}{\cosh(\varepsilon/k_{\mathrm{B}}T)+\cosh(E_{\mathrm{F}}/k_{\mathrm{B}}T)}.$$

Here $\sigma_0 = e^2/4\hbar$, $e$ — the elementary charge, $\hbar$ — Planck constant, $k_{\mathrm{B}}$ — Boltzmann constant, $\tau$ — time of dissipation

of the charge carriers, $\pm E_F$ — quasi Fermi levels, which define an inversion value of the charge carriers (electrons and holes) at the temperature $T$. The first summand in (1) characterizes intraband dissipative (Drude's) absorption in graphene as defined by the time $\tau$. The second summand characterizes interband transitions of the charge carriers in graphene. The presented expression does not include spatial dispersion of the conductivity. This is justified by the fact that the main interest of this study includes plasmons with low values of wave vectors and frequencies. This approximation was also used in other papers dedicated to similar structures [9,23,28].

Next, we will investigate a case in which TM-type waves propagate in the symmetric graphene structure. Let us represent a spatial & time dependence of magnetic and electric components of the single plasmon field in the three structure regions with the following equations:

$$H_z(t,x,y) = \exp[i(\omega t - k_x x)]H_z(y),$$

$$H_z(y) = \begin{cases} A_c \exp(k_{cy}|y|), & |y| > d/2, \\ A_b^- \exp(-k_{by}y) + A_b^+ \exp(k_{by}y), & |y| < d/2, \end{cases} \quad (2)$$

$$E_x = -\frac{1}{ik_0\varepsilon_b}\frac{\partial H_z}{\partial y}, \quad E_y = \frac{1}{ik_0\varepsilon_b}\frac{\partial H_z}{\partial x}, \quad (3)$$

where $k_x$ — plasmon propagation constant (PC), $k_0 = \omega/c$, $\omega$ and $c$ — frequency and speed of light in vacuum. For polaritons localized at the boundaries of the barrier layer (i.e. at the graphene sheets), transverse components of the wave vector in each of the media are represented as $k_{jy} = \sqrt{k_x^2 - \varepsilon_j\omega^2/c^2}$, where $j = b, c$ means the barrier layer and liners.

In order to find a dispersion equation of the waves propagating in the structure, it is necessary to supplement the relationships for the fields (2,3) with the following boundary conditions

$$E_{cx} = E_{bx}, \; H_{cz} - H_{bz} = \pm\frac{4\pi}{c}\sigma E_{cx} \; (y = \pm d/2). \quad (4)$$

Equating a determinant of the equation system (4) to zero, we come to the dispersion equation, which was obtained earlier in the paper [22]

$$\tanh(k_{by}d) = -\frac{2\psi}{1+\psi^2}, \quad \psi = \frac{k_{by}}{\varepsilon_b}\left(\frac{\varepsilon_c}{k_{cy}} + i\frac{4\pi\sigma}{\omega}\right). \quad (5)$$

Taking into account complex nature of parameters in this equation, it defines dependence of a PC real and imaginary part on the wave frequency. The equation (5) is split into two equations:

$$\tanh(k_{yb}\,d/2) = -1/\psi, \quad \tanh(k_{yb}\,d/2) = -\psi. \quad (6)$$

We name the modes, corresponding to the equation (6), symmetric ones (as per the paper [22]), while those corresponding to the equation (7) — antisymmetric ones. In accordance with the distribution $E_x$ — a component of the electric field of the TM-waves of the plasmons, which is tangential to the graphene layers relative to a structure reflection plane — this component is symmetric and antisymmetric for the corresponding modes. Below, we present results of numerical analysis of the equation for the antisymmetric plasma modes as obtained at the following values of the parameters: $\varepsilon_c = 1$, $T = 300$ K, $\tau = 1$ ps.

## 3. Calculation of dispersion dependences

The frequency dependence of the graphene conductivity (1) includes both dissipation mechanisms — Drude's intraband dissipative absorption and interband dissipation due to generation and recombination of electron-hole pairs. The Fig. 1 shows the dependence of the real and imaginary part of the conductivity on the frequency at the quasi-Fermi level's energy $E_F = 10, 30, 50, 70$ meV (the curves *1–4*). It is clear that the real part of the conductivity may be negative in a quite wide region of the terahertz range. Due to the radiative interband transitions in the said frequency region, the energy exceeds its total losses in graphene. The real part of the conductivity is positive outside this region (which corresponds to a mode of absorption in graphene), as at lower frequencies the intraband dissipative losses prevail, while at higher frequencies an energy quantum exceeds the double quasi-Fermi level's energy in the second summand of the formula (1). The imaginary part of the conductivity accounted for resonance frequencies of plasma oscillations in graphene is steadily changing in the whole frequency range under consideration.

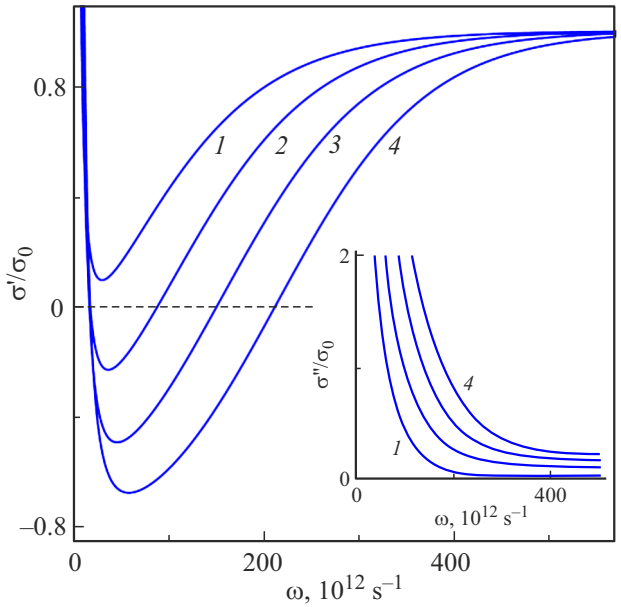


**Figure 1.** Dependence of the normalized real and imaginary part of the conductivity of the inverted graphene on the radiation frequency at the quasi-Fermi level's energy value $E_F = 10, 30, 50, 70$ meV (*1–4*).

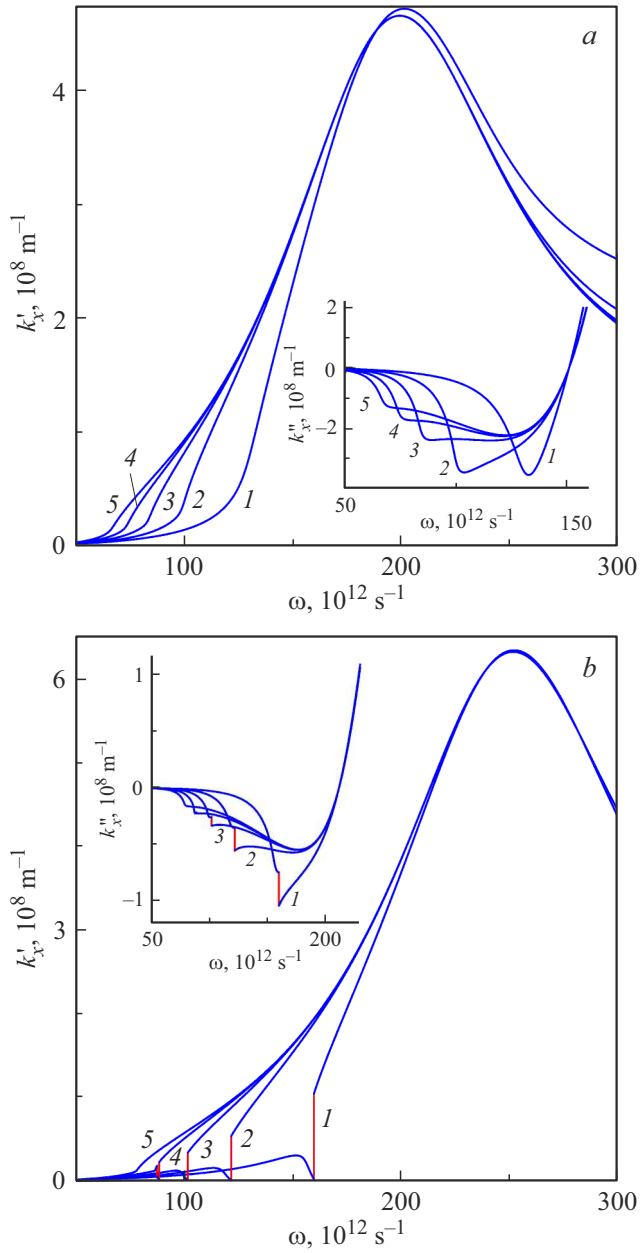


**Figure 2.** Dependences of plasmon PC components on the frequency at $E_F = 50$, 70 meV ($a, b$) and $\varepsilon_b = 10$ for the thicknesses $d = 10$, 20, 30, 40, 50 nm ($1-5$).

Next, we will consider the dependence of the real and imaginary plasmon PC part on the frequency. The Fig. 2 shows a general view of the dependences $k'_x(\omega)$ and $k''_x(\omega)$, which were obtained for the following values of the structure parameters: $E_F = 70$ meV, $\varepsilon_b = 10$, $d = 10$, 20, 30, 40, 50 nm (the curves $1-5$). It is clear from the figure that at $E_F = 50$ meV the dispersion dependences $k'_x(\omega)$ have a single maximum and are similar to those obtained for TM modes in the previous studies [10,20]. The situation is different at $E_F = 70$ meV: for quite small thicknesses of the barrier layer ($d < 50$ nm) there is also an evident additional maximum (besides the prominent maximum of the PC real part) to be followed by a substantial decrease in PC (to values smaller in order) and its abrupt increase thereafter. The presented figure (and hereinafter as well) depicts all numerically obtained solutions with blue dots (which are usually to be visually merged into a continuous line), while a line connecting the dots is red — in this way, it makes presence and absence of skipping more visible. The PC imaginary part is also undergoing an abrupt change at the same time. Note that in the case under consideration $k''_x$ is negative, i.e. the structure plasmons are undergoing gaining. With the increase in the barrier layer's thickness, the jump is shifting to the region of lower frequencies with decrease in its amplitude at the same time. And at quite big thicknesses (depending on $E_F$ and $\varepsilon_b$, as the calculations demonstrate) the dispersive jump is disappearing.

## 4. Bifurcation of the dispersion dependence and bistability

Despite the above solution is only for the equation of antisymmetric modes (7), the inconsiderate opinion makes the impression that the dispersive jump is attributed to the skipping between the different modes, whose dispersion curves approach closely to each other near the jump (the background thereof can be exemplified by roots and hyperbolic functions of a complex argument in the dispersion equation). Let us investigate in more detail a region of parameters near values corresponding to occurrence of the dispersive jump. The Fig. 3 shows the dependences $k'_x(\omega)$ and $k''_x(\omega)$ at $E_F = 70$ meV, $\varepsilon_b = 10$ for $d = 44$, 43, 42, 41, 40, 39, 38, 37.5, 37, 36.5, 36 nm (the curves $1-11$) — note that refinement of occurrence of the jump, as such, should predominantly focused on a mathematical aspect of the issue, rather than implementability of all selected values of the parameters.

It is clear from the figure that for the curve *1* no jump is observed, but for the curves $9-11$ the dependence $k'_x(\omega)$ starts smoothly decreasing before the jump, with the corresponding increase of the dependence $k''_x(\omega)$. In other cases, there are two main jumps: the dependences go away to another branch of solutions and return to an original branch, and with decrease of $d$, sections for implementation of the second branch are increasing at the same time. It should be noted that some sections have the red lines of the skipping thickened. It results from several closely adjacent skips due to bistability, i.e. one of the two solutions is implemented at the same parameters with the approximately equal probability.

Let us consider a progress of these dependences in more detail. The Fig. 4 marks out with blue color the increasing dependences $k'_x(\omega)$ of one branch of the solutions (and the respective decreasing dependences $k''_x(\omega)$), while the decreasing $k'_x(\omega)$ (and increasing $k''_x(\omega)$) dependences, corresponding to presumably another branch of the solutions — to which it comes off — are marked with green color. It is clear, however, that for the curves *8* and *9* the blue branches

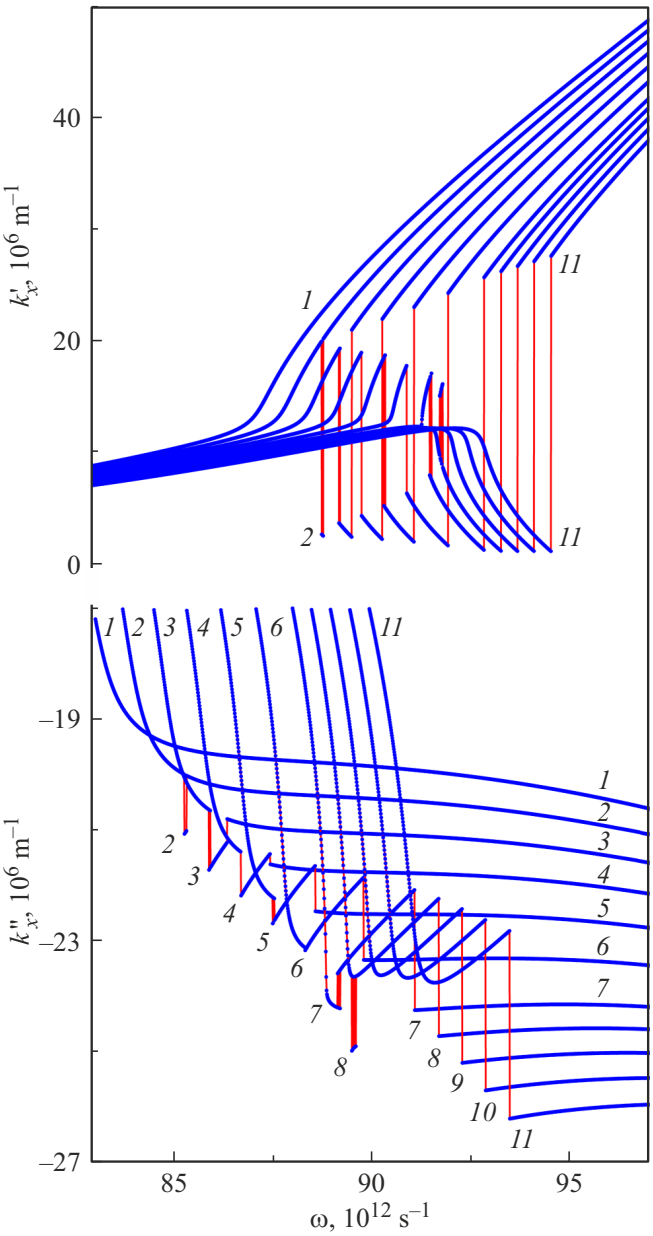


**Figure 3.** Dependences of plasmon PC components at $E_F = 70$ meV, $\varepsilon_b = 10$ for $d = 44$, 43, 42, 41, 40, 39, 38, 37.5, 37, 36.5, 36 nm (the curves *1–11*) — the numeric solutions are depicted with blue dots connected by red lines.

continuously go into the green ones, and they skip again to the blue branch at the end thereof! Thus, we are dealing not with two initially different branches of the solutions, but with bifurcation, at which one branch of the dispersion dependence is split into two branches of different stability and different probability of implementation, respectively (while in narrow regions, which have evident „thick red lines“ on the figure, these probabilities are approximately equal). It is obvious that the splitting bifurcation occurs within a region of a changing dependence progress, i.e. where a section close to the linear dependence ends. The

Figure (*a*) indicates with a dotted curve *3′* an approximate location of a branch unstable in a parametric space, which is occurring after the bifurcation (whose stability then changes). This situation is quite common in synergistic effects [29]. Discussing the process physics, we can state the following. In the two-layer graphene system under consideration, there is a situation, in which under a changing parameter the dispersion relationship derived based on the boundary conditions begins to be met with two combinations of the numbers $k'_x$ and $k''_x$ instead of one thereof — two modes occur differing in the PC real and imaginary part. As the dependence branches can be

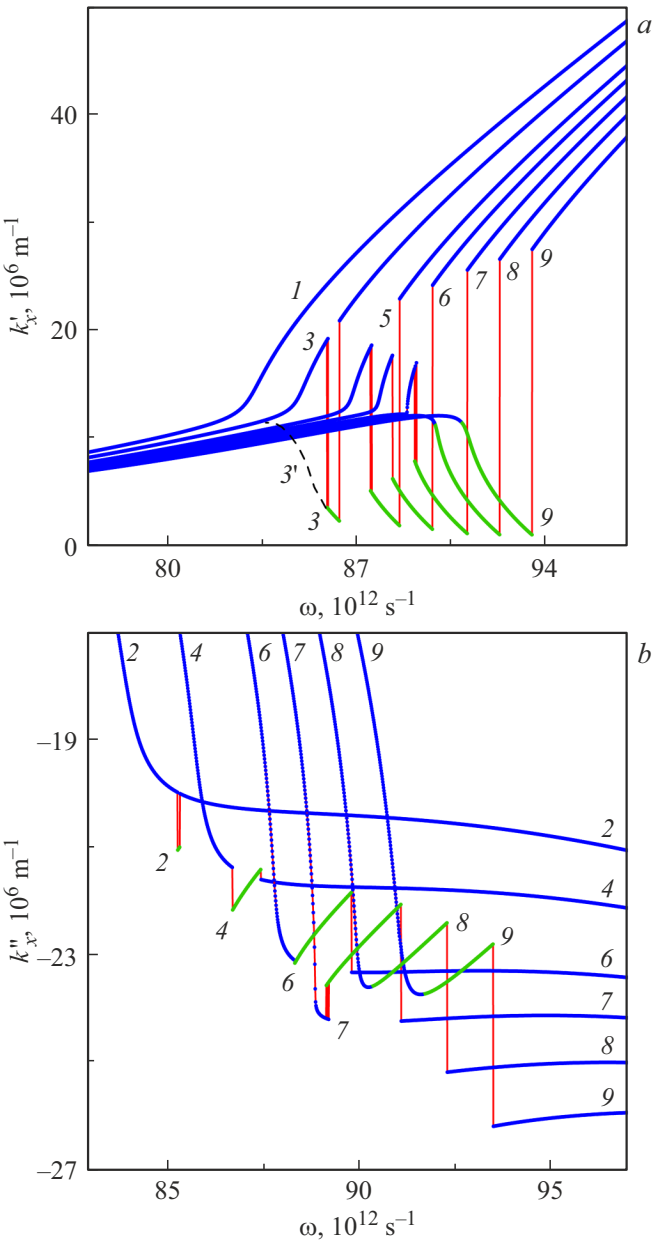


**Figure 4.** Occurrence of the modal bistability depending on the real and imaginary (*a, b*) plasmon PC components at $E_F = 70$ meV, $\varepsilon_b = 10$, $d = 44$, 43, 42, 41, 40, 39, 38, 37, 36 nm (the curves *1–9*).

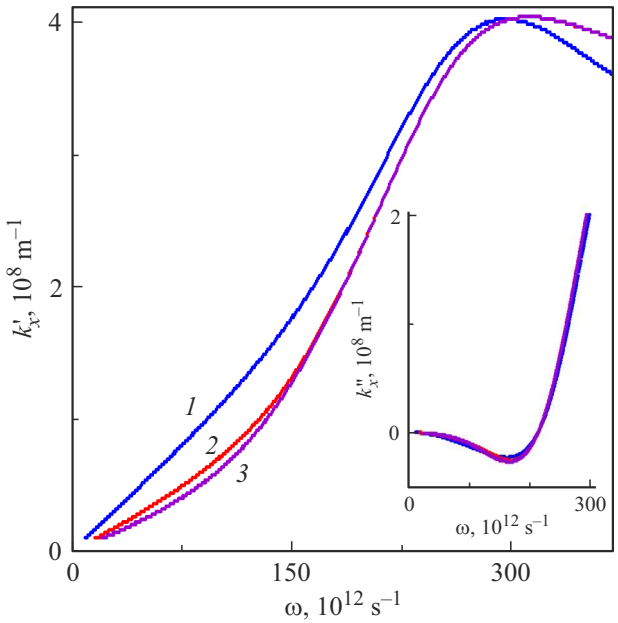


**Figure 5.** Dependences of PC components of the symmetric plasmon modes on the frequency at $E_F = 70$ meV and $\varepsilon_b = 10$ for the thicknesses $d = 10$, 30, 50 nm (*1–3*).

considered attractors with a different region of attraction, real systems having parameter fluctuations will have one mode related to a more stable branch out of the two modes corresponding to the bistability implemented (the numerical simulation reflects the specifics of the real process in this sense). If the system parameters are changing, then the stability of the bistability-related branches is changing, thereby leading to the evident dispersive jumps.

Additional studies have demonstrated that there is neither bifurcation, nor dispersive jumps in the dispersion dependence of the plasmon symmetric modes (6) under the parameters under consideration. The Fig. 5 shows the dependences of the PC components of the symmetric plasmon modes on the frequency at $E_F = 70$ meV and $\varepsilon_b = 10$ for the thicknesses $d = 10$, 30,50 nm (the curves *1–3*). The bifurcation of the dispersion dependence is essentially a synergistic effect present in the multi-layer structure under consideration. Thus, it is quite sensitive both to changing of parameters and a form of the equations under consideration.

## 5. Dependences on the thickness of the barrier layer

The dispersive jumps due to bistability occurred are also in the PC dependences on a refraction index or a thickness of the barrier layer. The respective splitting bifurcation of the plasmon dispersion branch occurs within a limited frequency range and at a quite big DP ($\varepsilon_b > 9$). The Fig. 6 shows the dependence of the real and imaginary plasmon PC component on $d$ at the frequencies $\omega = (0.8, 1.0, 1.2, 1.4, 1.6, 1.8) \cdot 10^{14}$ s$^{-1}$ (the curves *1–6*) for the parameters of the barrier layer and graphene $\varepsilon_b = 10$, $E_F = 70$ meV. Increase in DP $\varepsilon_b$ and the quasi-Fermi level energy leads to an extended interval of the barrier layer thicknesses, in which the jump of the dispersion dependences is implemented and to shifting its boundary to bigger $d$. The presented figure also shows that in all the cases the jump is before the dependences are constant, when mutual influence of the graphene layers becomes very small. It can be concluded that there is no effect under consideration in the systems with one graphene layer.

As in the previous section, let us consider occurrence of the dispersive jump and its disappearance. For $\varepsilon_b = 10$

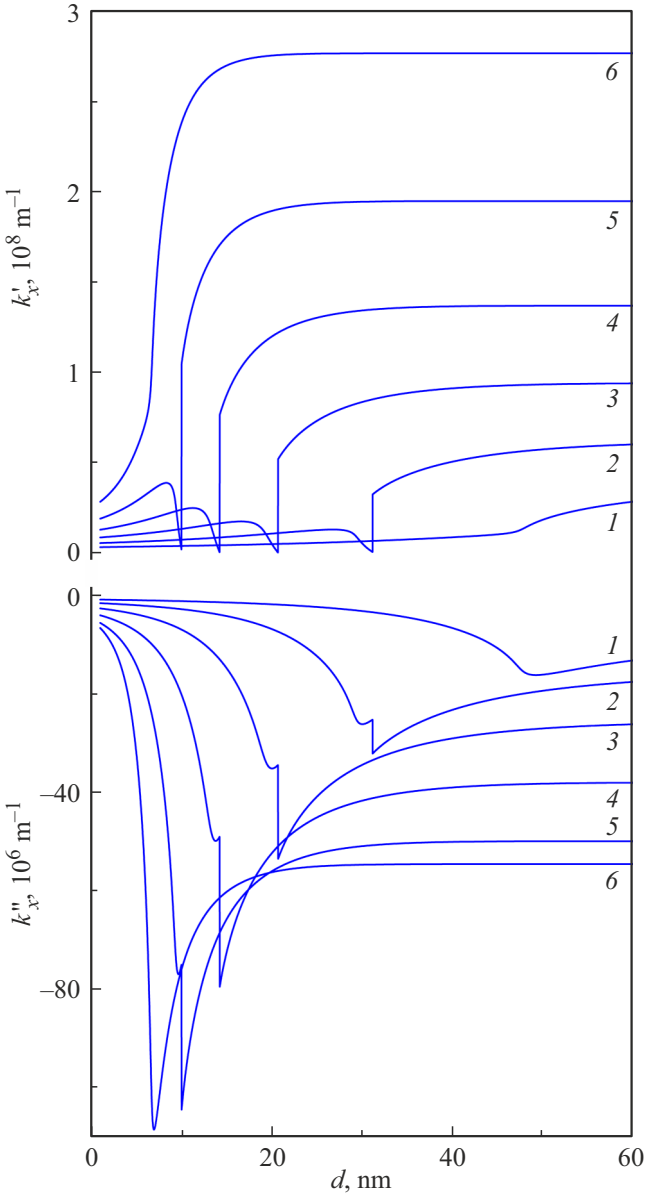


**Figure 6.** Dependence of the real and imaginary plasmon PC component on the barrier layer thickness for $\varepsilon_b = 10$, $E_F = 70$ meV at the frequencies $\omega = (0.8, 1.0, 1.2, 1.4, 1.6, 1.8) \cdot 10^{14}$ s$^{-1}$ (the curves *1–6*).

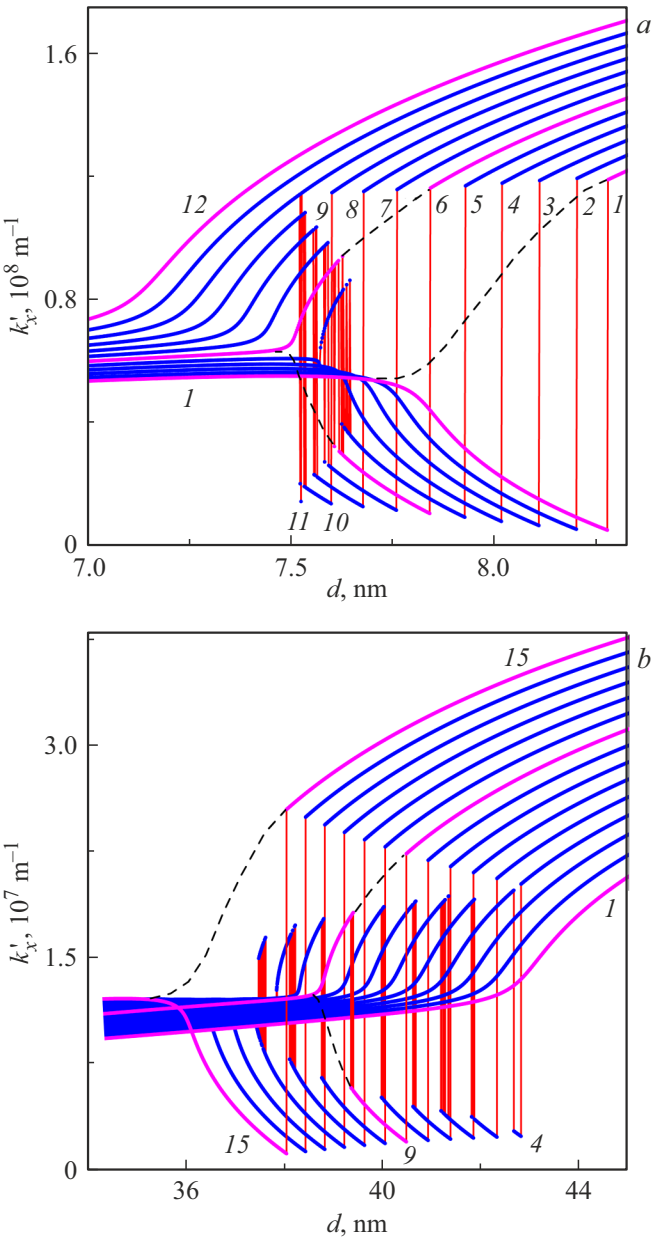


**Figure 7.** Dependence of the real PC plasmon component on the barrier layer thickness at the frequencies $\omega = (1.705 \div 1.76) \cdot 10^{14}\,\mathrm{s}^{-1}$ (*a*, the curves *1–12*) and $\omega = (0.84 \div 0.91) \cdot 10^{14}\,\mathrm{s}^{-1}$ (*b*, the curves *1–15*); $\varepsilon_b = 10$, $E_\mathrm{F} = 70$ meV.

and $E_\mathrm{F} = 70$ meV, the Fig. 7 shows the dependence of the real plasmon PC component on $d$ at the frequencies $\omega = (1.705 \div 1.76) \cdot 10^{14}\,\mathrm{s}^{-1}$ (*a*, the curves *1–12* — in equal $\Delta\omega$) and $\omega = (0.84 \div 0.91) \cdot 10^{14}\,\mathrm{s}^{-1}$ (*b*, the curves *1–15* — in equal $\Delta\omega$). The Fig. (*a*) shows evident occurrence of the splitting bifurcation of the dispersion branch when the frequency is decreasing. At the same time, first the lower branch (with lesser $k'_x$) turns out to be unstable. However, further decrease in the frequency leads to changing of stability of the branches and an extended interval, at which only the lower branch becomes stable. In each case, there is a critically low value $k'_x$, after which the lower branch loses stability and it jumps to the upper branch of the dispersion bistability. (Some sections of the dispersion dependences, which are unstable in a parametric space, are shown in a dashed line.) The Fig. *b* shows evident reverse bifurcation: when the frequency is decreasing, the two dispersion branches merge into one and the jump disappears. Note that the presented figure also has evident narrow sections (with thickened red lines), at which both branches of the dispersion bistability have near stability and are implemented with approximately equal probability. At the same time, the plasmonic modes related to different branches making up the bistability have a different gain increment and different phase and group velocities as well.

In the conclusion, note that the structure with doped graphene layers, in which the conductivity is determined using the formula as applied in the papers [27,31], was studied to demonstrate that there is also the bifurcation in the dispersion dependence in them, but at other values of the quasi-Fermi level. In particular, the structure with inverted graphene has the bifurcation and the respective bistability implemented at $E_\mathrm{F} = 70$, 90 meV, whereas for doped graphene — at $E_\mathrm{F} = 50$, 70 meV. For passive graphene, there is also the evident splitting bifurcation at the considered thicknesses of the barrier layer (however, in order to compare the dispersion at the said states of the structures, additional special studies are required). It means than this effect is somewhat general and observed in different states of the structure, uncritically depending on specific values of the graphene conductivity.

No detection of the presented effects in the previous studies of the similar structures [10,20,22,30] may be attributed to the fact that they are only in certain intervals of parameter values. Moreover, with a quite big step of parameter variation the specifics of the dispersion dependencies under consideration can be regarded as defects in numerical analysis.

## 6. Conclusion

For the plasmonic modes in the two-layer graphene structure the numerical analysis of the dispersion equation has demonstrated that at the quasi-Fermi level's energy $E_\mathrm{F} \geq 60$ meV and a quite thin barrier layer ($d \leq 50$ for $\varepsilon_b > 10$) there was the modal bistability and the dispersive jump of the real and imaginary plasmon PC part. This effect is caused by implementing the bifurcation of separation of one branch of the solutions to two branches, i.e. when the dispersion equation begins to be met with two sets of complex PC components. In the bistability occurred, usually, only one of the branches is stable (the unstable branch should also meet the dispersion equation, but because of a very narrow „region of attraction" in the parametric space it can not be virtually obtained numerically or experimentally). However, under a changing parameter

the stability of the branches changes and the region, in which the second branch limited by a minimum value of the real PC component becomes stable, is extended. When it is at that value, the stability returns to the first branch. In doing so, narrow parameter regions were detected, in which both branches included in the bistability are stable, i.e. in practice, both plasmonic modes will occur at approximately equal probability, differing in the gain increment, the phase velocity and having a different sign of their group velocities. The reverse bifurcation of joining two dispersion branches to one is also revealed.

The dispersive jump region has the following values therein $k'_x \sim 0.1\,\mathrm{Mm}^{-1}$, and $\Delta k'_x \sim 10\,\mathrm{Mm}^{-1}$. At the same time, the imaginary PC components remains negative $k''_x \sim -10\,\mathrm{Mm}^{-1}$, and, therefore, plasmon gaining is implemented. The increase in the Fermi energy and the barrier layer DP allows increasing the barrier layer thickness, at which there are the modal bistability and the dispersive jump. The additional studies have demonstrated that with the increase in the Fermi energy the periodicity of implementation of the splitting bifurcation shifted to higher values. The plasmon group velocities related to different dispersion branches included in the bistability are opposite in sign, which can be used for creating terahertz radiation generators based on two-layer graphene structures.

### Funding

This study was supported by Ministry of Science and Higher Education of the Russian Federation within the framework of the state assignment No. 0830-2020-0009.

### Conflict of interest

The authors declare that they have no conflict of interest.

## References

[1] K.S. Novoselov, A.K. Geim, S.V. Morozov, D. Jiang, M.I. Katsnelson, I.V. Grigorieva, S.V. Dubonos, A.A. Firsov. Nature **438**, 197 (2005).
[2] Y. Zhang, Y.-W. Tan, H.L. Stormer, P. Kim. Nature **438**, 201 (2005).
[3] E.M. Baitinger. Physics of the Solid State **48**, *8*, 1380 (2006).
[4] S.V. Morozov, K.S. Novoselov, A.K. Geim. UFN **178**, *7*, 776 (2008) (in Russian).
[5] L.A. Fal'kovsky. UFN **178**, *9*, 923 (2008) (in Russian).
[6] V.Ya. Aleshkin, A.A. Dubinov, V. Ryzhii. Pis'ma v ZhETF **89**, 70 (2009).
[7] A.H. Castro Neto, F. Guinea, N.M.R. Peres. Rev. Mod. Phys. **81**, 109 (2009).
[8] S. Das Sarma, S. Adamet, E.H. Hwang, E. Rossi. Rev. Mod. Phys. **83**, *2*, 407 (2011).
[9] V.V. Popov, O.V. Polischuk, A.R. Davoyan, V. Ryzhii, T. Otsuji, M.S. Shur. Phys. Rev. B **86**, 195437 (2012).
[10] I.V. Iorsh, I.V. Sharidov, P.A. Belov, Yu.S. Kivshar. Pis'ma v ZhETF **97**, 287 (2013).
[11] D.A. Smirnova, P.I. Buslaev, I.V. Iorsh, I.V. Shadrivov, P.A. Belov, Y.S. Kivshar. Phys. Rev. B **89**, 245414 (2014).
[12] A.S. Abramov, D.A. Evseev, D.I. Sementsov. Opt. i spektr. **124**, *2*, 235 (2018) (in Russian).
[13] V. Ryzhii, M. Ryzhii, T. Otsuji. J. Appl. Phys. **101**, 083114 (2007).
[14] A. Satou, F.T. Vasko, V. Ryzhii. Phys. Rev. B **7**, 1158431 (2008).
[15] A.A. Dubinov, V.Y. Aleshkin, M. Ryzhii, T. Otsuji, V. Ryzhii. Appl. Phys. Exp. **2**, 092301 (2009).
[16] A. Satou, V. Ryzhii, Y. Kurita, T. Otsuji. J. Appl. Phys. **113**, 143108 (2013).
[17] N.N. Yanyushkina, M.B. Belonenko, N.G. Lebedev. Opt. i spektr. **108**, *4*, 658 (2010) (in Russian).
[18] A.A. Dubinov, V.Y. Aleshkin, V.V. Mitin, T. Otsuji, V. Ryzhii. Phys.: Condens. Matter. **23**, 145302 (2011).
[19] F. Rana. IEEE Trans. Nanotechn. **7**, 91 (2008).
[20] P.I. Buslaev, I.V. Iorsh, I.V. Shadrivov, P.A. Belov, Yu.S. Kivshar. Pis'ma v ZhETF **97**, *9*, 619 (2013) (in Russian).
[21] C.H. Gan, H.S. Chu, E.P. Li. Phys. Rev. B **85**, 125431 (2012).
[22] M.Yu. Morozov, I.M. Moiseenko, V.V. Popov. Izv. Saratov. un-ta. Nov. ser. Ser. Fizika. **19**, *1*, 28 (2019) (in Russian).
[23] O.V. Polischuk, D.V. Fateev, V.V. Popov. FTP **53**, *9*, 1237 (2019) (in Russian).
[24] E.I. Kukhar', S.V. Kryuchkov. Physics of the Solid State **62**, *1*, 153 (2020).
[25] A.R. Davoyan, M.Yu. Morozov, V.V. Popov, A. Satou, T. Otsuji. Appl. Phys. Lett. **103**, 251102 (2013).
[26] M.Yu. Morozov, A.R. Davoyan, I.M. Moiseenko, A. Satou, T. Otsuji, V.V. Popov. Appl. Phys. Lett. **106**, 061105 (2015).
[27] L.A. Falkovsky, A.A. Varlamov. Eur. Phys. J. B **56**, 281 (2007).
[28] M.Yu. Morozov, I.M. Moiseenko, A.V. Korotchenkov, V.V. Popov. FTP **55**, *6*, 518 (2021) (in Russian).
[29] D.I. Sementsov, A.M. Shutyi. UFN **177**, *8*, 831 (2007) (in Russian).
[30] M.Yu. Morozov, I.M. Moiseenko, V.V. Popov. J. Phys.: Condens. Matter **30**, 08LT02 (2018).
[31] O.V. Polischuk, D.V. Fateev, V.V. Popov. FTP **52**, *12*, 1430 (2018) (in Russian).